Inorg. Chem. **2003**, *42*, 8524–8533

Low-Temperature Single-Crystal Raman and Neutron-Diffraction Study of the Hydrogenous Ammonium Copper(II) Tutton Salt and the Deuterated Analogue in the Metastable State

Christopher Dobe, Graham Carver, Hans-Beat BÜrgi, and Philip L. W. Tregenna-Piggott*

Department of Chemistry and Biochemistry, University of Bern, Freiestrasse 3, CH-3000, Bern 9, Switzerland

Garry J. McIntyre*

Institut Laue-Langevin, BP156, 38042 Grenoble, Cedex 9, France

Maria A. Augustyniak-Jablokow

Polish Academy of Sciences, Institute of Molecular Physics, Smoluchowskiego 17, 60-179 Poznan, Poland

Mark J. Riley

Department of Chemistry, School of Molecular and Microbial Sciences, The University of Queensland, Brisbane, Queensland, Australia, 4072

Received April 1, 2003

Low-temperature (15 K) single-crystal neutron-diffraction structures and Raman spectra of the salts $(NX_4)_2[Cu(OX_2)_6](SO_4)_2$, where X = H or D, are reported. This study is concerned with the origin of the structural phase change that is known to occur upon deuteration. Data for the deuterated salt were measured in the metastable state, achieved by application of 500 bar of hydrostatic pressure at ~303 K followed by cooling to 281 K and the subsequent release of pressure. This allows for the direct comparison between the hydrogenous and deuterated salts, in the same modification, at ambient pressure and low temperature. The Raman spectra provide no intimation of any significant change in the intermolecular bonding. Furthermore, structural differences are few, the largest being for the long Cu–O bond, which is 2.2834(5) and 2.2802(4) Å for the hydrogenous and the deuterated salts, respectively. Calorimetric data for the deuterated salt are also presented, providing an estimate of 0.17(2) kJ/mol for the enthalpy difference between the two structural forms at 295.8(5) K. The structural data suggest that substitution of hydrogen for deuterium gives rise to changes in the hydrogen-bonding interactions that result in a slightly reduced force field about the copper(II) center. The small structural differences suggest different relative stabilities for the hydrogenous and deuterated salts, which may be sufficient to stabilize the hydrogenous salt in the anomalous structural form.

1. Introduction

The ammonium copper(II) Tutton salt, $(NH_4)_2[Cu(OH_2)_6](SO_4)_2$, exhibits remarkable physical properties, which have been the focus of a number of notable articles in recent years.[1−5] Both the ground-state *g* values and the stereochemistry of the $[Cu(OH_2)_6]^{2+}$ cation are strongly temperature dependent,[6,7] and this has been rationalized using various Jahn−Teller coupling models.[7−9] Perhaps the most fascinating aspect of the structural chemistry is the fact that the hydrogenous salt (modification B) undergoes a structural change upon deuteration[1] (to modification A). Modification B of the hydrogenous salt is anomalous in the copper(II) Tutton salt series. In both salts, the CuO_6 framework adopts

* Authors to whom correspondence should be addressed. E-mail: tregenna@iac.unibe.ch (P.L.W.T-P.); mcintyre@ill.fr (G.J.M.).

10.1021/ic0343511 CCC: $25.00
Published on Web 11/08/2003

an approximately tetragonal elongated geometry, with the structures differing in terms of the identity of the longest Cu−O bond with respect to the crystallographic axes. Specifically (adopting the labeling scheme of ref 2), upon deuteration the longest bond, Cu−O(7), switches with the medium bond, Cu−O(8), whereas the shorter Cu−O(9) bond remains invariant. This article is concerned with the origin of the structural difference between the hydrogenous and deuterated salts.

Neutron and X-ray diffraction studies have been reported on both hydrogenous and deuterated salts as a function of temperature and pressure.[1,2,7,10−14,16] It was during the pursuit of crystallographic neutron data that the isotopically induced structural change was first noted.[1] Temperature-dependent studies suggest an averaging of the Cu−O(7) and Cu−O(8) bond lengths at temperatures above ∼150 K,[1,7] an observation corroborated by numerous electron paramagnetic resonance (EPR) investigations.[6−8] Extended X-ray absorption fine structure (EXAFS) experiments showed that the local Cu−O bond lengths do not actually change significantly with temperature.[15] This arises because the electronic and geometric properties of the $[Cu(OH_2)_6]^{2+}$ cation, determined by a given experimental technique, depend on both the time scale of the experiment and whether the local or space-averaged property is being determined.[15]

An early synchrotron X-ray diffraction study followed the Bragg peak shape of several reflections as a function of temperature.[16] The conclusion that there were temperature-dependent domains present was a harbinger of later interpretations involving cooperative effects.[7] The first work to employ pressure clearly demonstrated that application of hydrostatic pressure to the deuterated salt leads to the adoption of the hydrogenous structure.[2] In this seminal study, data were collected for the deuterated salt at 15 K, after which the sample was warmed to room temperature, pressurized to 1.5 kbar, and cooled back to 15 K for the high-pressure collection. The high-pressure structure was shown to be analogous to that obtained for the hydrogenous salt under the same conditions. It was subsequently shown that irradiation of an N−D vibrational band in the infrared can also induce localized switching to the hydrogenous form.[17]

From pressure-dependent X-ray diffraction measurements on the deuterated salt, an estimate of 0.18(3) kJ/mol for the energy difference between modifications A and B was obtained.[18] A further experiment involving neutron powder diffraction and EPR[19] followed the structural changes as a function of pressure, to provide the most detailed crystallographic observations of the transition. Although the number of reflections collected at each pressure was limited, hysteresis of the pressure-induced Jahn−Teller switch was demonstrated, and the 295 K transition pressure was refined to ∼240 bar. In a single-crystal EPR study,[5] the pressure at which the structural transition is induced was shown to be highly dependent on the temperature, with the required pressure increasing from 240 bar at 295 K to 4.5 kbar at 150 K. It was observed that the high-pressure phase of the deuterated salt is metastable after the pressure is released, provided the temperature remains below 297 K.[5] The most recent pressure work involved a further neutron powder study,[20] from which the enthalpy change which accompanies the transition was determined to be 0.34 kJ/mol at 303 K The enthalpy change increases steadily as the temperature is decreased and reaches a value of 3.1 kJ/mol at 260 K.

Further aspects of the isotopically induced transition have been studied. The two structures switch close to 50% deuteration,[3] whereas isotopic substitution with ^{18}O enriched water, which yields the same mass change in the ligated water, revealed no structural variations.[21] It was suggested that the isotopically induced transition must be related to changes in the hydrogen-bonding interactions, which alter the lattice-strain interactions acting upon the copper(II) complex ion.[21] Despite the large body of work, there is as yet no conclusive explanation as to the origin of the structural difference between the hydrogenous and deuterated salts.

Structural changes upon deuteration may be found in other compounds, a notable example being trifluoroacetic acid tetrahydrate, which is cationic in the protonated form but becomes molecular when deuterated.[22] Structural anomalies in salts containing transition-metal complexes with degenerate ground terms are also not uncommon. Among the clearest and best-understood examples are the vanadium(III) alums of formula $[M^I(OH_2)_6][V(OH_2)_6](SO_4)_2$, where M^I is Rb or K.[23,24] The structures of these salts differ markedly from those usually found for the other Rb and K alums, and this has

(1) Hathaway, B. J.; Hewat, A. W. *J. Solid State Chem.* **1984**, *51*, 364.
(2) Simmons, C. J.; Hitchman, M. A.; Stratemeier, H.; Schultz, A. J. *J. Am. Chem. Soc.* **1993**, *115*, 11304.
(3) Henning, R. W.; Schultz, A. J.; Hitchman, M. A.; Kelly, G.; Astley, T. *Inorg. Chem.* **2000**, *39*, 765.
(4) Simmons, C.; Hitchman, M. A.; Stratemeier, H.; Astley, T. *Inorg. Chem.* **2000**, *39*, 4651.
(5) Augustyniak, M. A.; Krupski, M. *Chem. Phys. Lett.* **1999**, *311*, 126.
(6) Marciniak, M.; Hoffmann, S. K.; Augustyniak, M. A.; Hilczer, W. *Phys. Status Solidi B* **1995**, *191*, 201.
(7) Hitchman, M. A.; Maaskant, W.; van der Plas, J; Simmons, C. J.; Stratemeier, H. *J. Am. Chem. Soc.* **1999**, *121*, 1488.
(8) Riley, M. J.; Hitchman, M. A.; Mohammed, A. W. *J. Chem. Phys.* **1987**, *87* (7), 3766.
(9) Silver, B. L.; Getz, D. *J. Chem. Phys.* **1978**, *61*, 638.
(10) Figgis, B. N.; Khor, L.; Kucharski, E. S.; Reynolds, P. A. *Acta Crystallogr., Sect. B* **1992**, *48*, 144.
(11) Alcock, N. W.; Duggan, M.; Murray, A.; Tyagi, S.; Hathaway, B. J.; Hewat, A. *J. Chem. Soc., Dalton Trans.* **1984**, 7.
(12) Montgomery, H.; Lingafelter, E. *Acta Crystallogr.* **1966**, *20*, 659.
(13) Brown, G. M.; Chidambaram, R. *Acta Crystallogr., Sect. B* **1969**, *25*, 676.
(14) Maslen, E. N.; Watson, K. J.; Moore, F. H. *Acta Crystallogr., Sect. B* **1988**, *44*, 102.
(15) Masters, V. M.; Riley, M. J.; Hitchman, M. A. *Inorg. Chem.* **2001**, *40*, 843.
(16) Figgis, B. N.; Reynolds, P. A.; Hanson, J. C.; Mutikainen, I. *Phys. Rev. B* **1993**, *48* (18), 13372.
(17) Cha, Y. H.; Strauss, H. L. *J. Phys. Chem. A* **2002**, *106*, 3531.
(18) Rauw, W.; Ahsbahs, H.; Hitchman, M. A.; Lukin, S.; Reinen, D.; Schultz, A. J.; Simmons, C. J.; Stratemeier, H. *Inorg. Chem.* **1996**, *35*, 1902.
(19) Schultz, A. J.; Hitchman, M. A.; Jorgensen, J. D.; Lukin, S.; Radaelli, P. G.; Simmons, C. J.; Stratemeier, H. *Inorg. Chem.*, **1997**, *36*, 3382.
(20) Schultz, A. J.; Henning, R. W.; Hitchman, M. A.; Stratemeier, H. *Cryst. Growth & Des.*, in press.
(21) Figgis, B. N.; Sobolev, A. N.; Simmons, C. J.; Hitchman, M. A.; Stratemeier, H.; Riley, M. J. *Acta Crystallogr., Sect. B* **2000**, *56*, 438.
(22) Mootz, D.; Schilling, M. *J. Am. Chem. Soc.* **1992**, *114*, 7435.
(23) Beattie, J. K.; Best, S. P.; Del Favero, P.; Skelton, B. W.; Sobolev A. N.; White, A. H. *J. Chem. Soc., Dalton Trans.* **1996**, 1481.
(24) Tregenna-Piggott, P. L. W.; Best, S. P. *Inorg. Chem.* **1996**, *35*, 5730.

been attributed to differences in the electronic stabilization energy, associated with two structural modifications. If the vanadium alum were to adopt the more usual structural modification, the $[V(OH_2)_6]^{3+}$ cation would be constrained, by hydrogen bonding, from distorting along the coordinate that leads to a significant stabilization of the ^3A_g (S_6) ground term. Such considerations are all the more important for salts containing octahedrally coordinated copper(II) complexes, where the Jahn−Teller stabilization energy is considerable. Ab initio calculations performed on the $[Cu(OH_2)_6]^{2+}$ cation and the $[Cu(OH_2)_6]^{2+}\cdot 12H_2O$ cluster are particularly useful, as they attempt to account for the effect of hydrogen bonding in crystalline hydrates.[25] The results suggest that the mean Cu−O bond length and the magnitude of the Jahn−Teller distortion are both strongly dependent on the polarization of the first coordination sphere by hydrogen bonding. Differences in hydrogen bond lengths between hydrogenous and deuterated structures are well documented; Rundle has provided a very readable account of the origin of the isotope effect.[26] Does deuteration instigate a change in the hydrogen bonding of the ammonium copper Tutton salt that is significant enough to alter the Jahn−Teller stabilization energy of the $[Cu(OH_2)_6]^{2+}$ cation? It was with this question in mind that the experimental work presented in this article was pursued. The observation that the deuterated salt may be prepared in the metastable state forms the basis for the present study, as this allows for the direct comparison of the hydrogenous and deuterated structures, in form B, at ambient pressure, without the physical constraints imposed by pressure cells. The measurements were conducted at ∼15 K. At this temperature the stereochemistry of the $[Cu(OH_2)_6]^{2+}$ cation in $(NH_4)_2[Cu(OH_2)_6](SO_4)_2$ is localized in the configuration of minimum energy, and the Jahn−Teller stabilization energy may be related to the low-temperature geometry.

Raman and crystallographic data are presented for the hydrogenous salt in modification B, and for the deuterated salt in modifications A and B, at ambient pressure. The data suggest that the intra- and intermolecular bonding in modification B of the hydrogenous and deuterated salts are very similar. Nevertheless, the small differences that are observed do suggest changes in some of the hydrogen-bonding interactions and in the E⊗e potential energy surface of the $[Cu(OH_2)_6]^{2+}$ complex. The discussion focuses on the relationship between small structural differences and the overall stabilities of the salts.

2. Experimental Section

2.1. Synthesis. $(ND_4)_2SO_4$ was prepared by recrystallizing $(ND_4)_2SO_4$ twice in a minimum of hot D_2O. $(ND_4)_2Cu(OD_2)_6(SO_4)_2$ was prepared by the dissolution of stoichiometric quantities of $(ND_4)_2SO_4$ and $CuSO_4$ (anhydrous) in hot D_2O. The resulting solution was cooled to 2° C, to allow crystallization of the salt. Approximately 40 g of the collected material was added to ∼140 mL of D_2O in a crystal-growing apparatus maintained at ∼5° C. A significant portion of the material remained undissolved. A 5° C temperature gradient was then created across the apparatus, and a seed crystal, mounted on a drawn glass fiber, was suspended in the solution. A constant stream of argon bubbles assisted in the transport of material to the seed crystal, as well as providing a H_2O-free atmosphere for the deuterated salt. The hydrogenous salt was prepared in an analogous manner. Crystals were allowed to grow for periods varying between 2 days and a week, depending on the required crystal size.

2.2. Collection of Neutron-Diffraction Data. Single-crystal neutron-diffraction data were collected on the four-circle diffractometer D9 at the Institut Laue-Langevin, Grenoble. A neutron beam of wavelength $\lambda = 0.8231(1)$ Å, obtained by reflection from a Cu (220) monochromator, was used. To facilitate the comparison of the two structures, the data for each of the two salts were collected consecutively, without change of wavelength. Therefore, the uncertainty in the wavelength does not play a role in evaluating *relative* differences in unit-cell parameters and hence bond lengths. Furthermore, for this experiment D9 was equipped with a small two-dimensional area detector[27] whose primary advantage was to allow optimal delineation of the peak from the considerable incoherent background from hydrogen in the case of $(NH_4)_2Cu(OH_2)_6(SO_4)_2$. In addition, because the three-dimensional count distribution around each reflection was observed, the centroids of all scanned reflections could be found[28] and *all* reasonably strong reflections used to estimate very precisely the (relative) unit-cell parameters for both compounds.

A single, transparent, pale-blue $(ND_4)_2Cu(OD_2)_6(SO_4)_2$ crystal (37.2 mg, 3.0 × 2.2 × 2.6 mm^3) was wrapped in fine aluminum foil, attached to a vanadium pin, transferred to a helium pressure cell at ∼303 K, and pressurized to 500 bar. The crystal was then cooled to 281 K, returned to ambient pressure, and then transferred to the precooled D9 Displex cryorefrigerator, where it was cooled further to 15 K. Unit-cell parameters were refined using the program RAFD9. Reflections were measured up to $2\theta = 80°$, giving a total of 3340 observations. Unit-cell parameters $a = 9.1025(2)$ Å, $b = 12.2289(3)$ Å, $c = 6.3599(2)$ Å, $\beta = 106.290(2)°$, in the space group $P2_1/a$, were obtained, using 2092 strong reflections, giving a cell volume of $V = 679.52(8)$ Å^3. The data were corrected for background,[28] absorption ($\rho = 0.1403$ cm^{-1}), and multiple scattering, the latter estimated from the small, nearly uniform observed intensities of reflections which should be systematically absent.[29,30] Structural refinements were performed with the program SFLSQ, which is based on the Cambridge crystallographic subroutine library (CCSL).[31] The scattering length of deuterium was kept as a variable to account for incomplete deuteration. The obtained value of 6.60(3) fm equates to 99.3% deuteration. Refining on F with 2489 reflections resulted in $\chi^2 = 4.52$. The moderate extinction could be well corrected by a Becker and Coppens[32,33] isotropic type 1 Lorentzian model. Bond lengths and angles were calculated using Parst97.[34]

A single, perfectly transparent, slightly deeper-blue $(NH_4)_2Cu(OH_2)_6(SO_4)_2$ crystal (11.2 mg, 1.4 × 1.2 × 2.6 mm^3) was mounted

(25) Åkessom, R.; Pettersson, L. G. M.; Sandström, M.; Wahlgren, U. *J. Phys. Chem.* **1992**, *96*, 150.
(26) Rundle, R. E. *J. Phys.* **1964**, *25*, 487.
(27) Lehmann, M. S.; Kuhs, W. F.; McIntyre, G. J.; Wilkinson, C.; Allibon, J. R. *J. Appl. Crystallogr.* **1989**, *22*, 562.
(28) Wilkinson, C.; Khamis, H. W.; Stansfield, R. F. D.; McIntyre, G. J. *J. Appl. Crystallogr.* **1988**, *21*, 471.
(29) Le Page, Y.; Gabe, E. J. *Acta Crystallogr.* **1979**, *A35*, 73.
(30) Luzon, J.; Dobe, C.; McIntyre, G. J. Personal communication.
(31) Matthewman, J. C.; Thompson, P.; Brown, P. J. *J. Appl. Crystallogr.* **1982**, *15*, 167.
(32) Becker, P.; Coppens, P. *Acta Crystallogr.* **1974**, *A30*, 129.
(33) Becker, P.; Coppens, P. *Acta Crystallogr.* **1975**, *A31*, 417.
(34) Nardelli, M. *J. Appl. Crystallogr.* **1995**, *28*, 659.

Table 1. Data Collection and Analysis Parameters for Measurements Performed on the Four-Circle Single-Crystal Neutron-Diffractometer D9

Crystal Data

	hydrogenous	deuterate
chemical formula	$(NH_4)_2Cu(H_2O)_6(SO_4)_2$	$(ND_4)_2Cu(D_2O)_6(SO_4)_2$
fw (g)	400	420
T (K)	15	15
cell setting	monoclinic	monoclinic
space group	$P2_1/a$	$P2_1/a$
a (Å)	9.1091(3)	9.1025(2)
b (Å)	12.2354(4)	12.2289(3)
c (Å)	6.3611(3)	6.3599(2)
β (deg)	106.308(3)	106.290(2)
V (Å^3)	680.44(11)	679.52(8)
wavelength (Å)	0.8231(1)	0.8231(1)
Z	2	2
no. of reflns for cell params	966	2092
θ range (deg)	4−45	4−40
μ (cm^{-1})	2.266	0.1403
cryst form	rectangular	octahedron
cryst size (mm^3)	4.4	17.16
cryst color	pale blue	pale blue
data collection method	$\omega - x\theta$ scans	$\omega - x\theta$ scans
no. of measured reflns	3209	3340
no. of independent reflns	2366	2489
R_{int}	0.026	0.018
θ_{max} (deg)	46	40
range of h, k, l	−15 to 13	−14 to 10
	−10 to 19	−10 to 19
	0 to 9	−1 to 9
no. of standard reflns	1	1
frequency of standard	every 50 reflns	every 100 reflns

Refinement

	hydrogenous	deuterate
refinement on	F	F
$R(F)$	0.034	0.018
$wR(F)$	0.022	0.018
S	1.44	2.13
no. of reflns used in refinement	2366	2489
no. of params used	179	180
weighting scheme (all data)	$w = 1/[\max(\sigma^2(F_o^2), \sigma_{pop}(F_o^2)]$	
extinction method (all data)	Lorentzian type 1 isotropic	
extinction coefficient (10^{-4} rad^{-1})	0.310(9)	0.334(4)
source of atomic scattering factors (all data)	Sears (1986)	

Computer Programs

data collection (all data)	MAD
cell refinement (all data)	RAFD9
data reduction (all data)	RACER
	CCSL
structure refinement (all data)	SFLSQ (based on CCSL)

as above and cooled to 15 K. Data were again collected under the same conditions to give a total of 3311 observations. Unit-cell parameters were refined to $a = 9.1091(3)$ Å, $b = 12.2354(4)$ Å, $c = 6.3611(3)$ Å, $\beta = 106.308(3)°$, and $V = 680.44(11)$ Å^3 using 966 strong reflections. As above, the data were corrected for background, absorption ($\rho = 2.266$ cm^{-1}), and multiple scattering. Refining on F gave $\chi^2 = 2.07$. Experiment and refinement details for both crystals are summarized in Table 1.

2.3. Collection of Raman Spectra. For Raman spectroscopy cubes of approximately 4 × 4 × 4 mm were cut with a diamond saw from large single crystals of known morphology.[35] The faces were chosen so as to be orthogonal to the optic axes, as determined by a polarizing microscope. Only the b crystallographic axis is coincident with an optic axis. The cubes were then ground and polished with 10, 1, and 0.3 μm Al_2O_3 before mounting with Araldite on the sample space goniometer. The crystals were attached on the crystallographic ab face with the b axis vertical to the scattering plane. The incident laser beam was along the a axis, and Raman scattering was observed from the ab face (c^* axis).

A He-gas pressure cell was constructed, based on a previous design,[36] so as to accommodate the goniometer preloaded with a $(ND_4)_2Cu(OD_2)_6(SO_4)_2$ crystal. Pressure was applied to 450 bar at room temperature and maintained while the pressure cell was cooled in ice for 20 min, before being slowly released. The pressure cell was then placed in a Dewar flask with dry ice for transport. Final loading onto the sample rod was performed in a cold room at 277 K, before insertion into the precooled cryostat and further cooling to 15 K.

Single-crystal Raman spectra were collected in a 90° geometry utilizing a Spectra Physics 2060-10 Ar^+ laser, an Oxford Instruments helium optical cryostat, and a Spex 1402 double monochromator. The 514.5 or 457 nm laser line was utilized with 50 mW power at the sample. The incident beam was passed through a

(35) Tutton, A. E. H. *Philos. Trans. R. Soc. London, Ser. A* **1916**, *216*, 1.

(36) Jeftic, J.; Kindler, U.; Spiering, H.; Hauser, A. *Meas. Sci. Technol.* **1997**, *8*, 479.

dispersion prism, polarization rotator, pinhole, and 50 mm achromatic focusing lens. The scattered light was collected using a 50 mm f1.2 Canon photographic lens followed by a Polaroid-film analyzer, a 90° image rotator,and finally a quartz-wedge scrambler. The monochromator was fitted with 1800 lines/mm holographic gratings and a Peltier-cooled RCA C31034 photomultiplier with associated Stanford-Instruments photon counter. Typical monochromator settings were slits of 150−170−150 μm, 0.009 nm steps to 1200 cm^{-1}, and 0.027 nm steps to 4000 cm^{-1}. Count times of 1 to 4 s per step were employed, depending on the crystal size and quality. Under routine conditions the above setup allowed the excitation line to be approached to within 10 cm^{-1}.

2.4. Collection of Differential Scanning Calorimetry Data. Small regular off-cuts from the Raman sample preparation were used for differential scanning calorimetry (DSC). DSC measurements were performed on a Mettler DSC25 Star^e system with a methodology similar to that previously employed in the study of quenched metastable phases.[37] The instrument was calibrated against an In standard. Deuterated single-crystals switched to form B were placed in 40 μL aluminum cans and heated from 293 to 296.5 K at a rate of 0.5 K/min and 10 data points per second.

3. Results

3.1. Raman Spectra. Vibrational spectroscopy has been established as a very sensitive probe of intra- and intermolecular bonding in crystalline hydrates. In particular, the alum double salts of general formula $M^{I}M^{III}(OH_2)_6(SO_4)_2 \cdot 6H_2O$ have been subject to numerous low-temperature single-crystal Raman measurements, which facilitates a complete assignment in the spectral region of 10−1200 cm^{-1}.[38−41] It was shown that small structural differences manifest in very notable changes in the Raman spectrum.

Single-crystal Raman studies have been reported for several Tutton salts.[42−52] These Raman spectra were obtained almost exclusively at room temperature. Hence, the bands are very broad and the resolution is poor. This, coupled with the low symmetry of the crystal system, has rendered the assignment of the vibrational spectrum of uncertain reliability. In view of the resurgence of interest in this crystal system, we have conducted a number of single-crystal Raman measurements on the Tutton salts, and some results are presented in this paper.

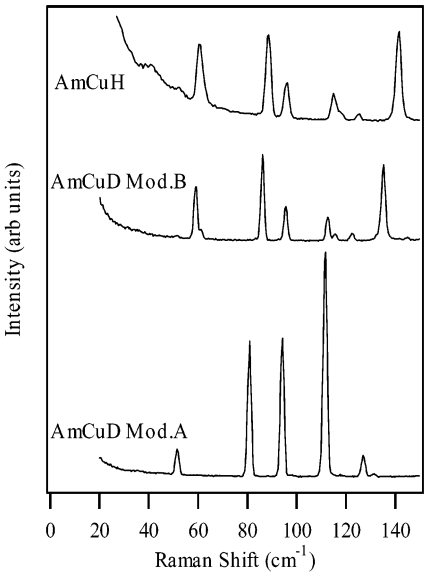

Figure 1. Single-crystal Raman spectra of ammonium copper sulfate (AmCu) in the hydrogenous (H) and deuterate (D) A and B forms: collected at 15 K; spectra normalized to the ν_1SO_4 band; polarization $X(ZZ)Y$ selecting for bands of A_g symmetry. A step size of 0.029 nm with 514.5 nm excitation and 50 mW power at the sample was used. The spectral bandwidth was 1.5 cm^{-1} in the displayed range and 1.9 cm^{-1} in the hydrogenous spectra (due to a larger slit width).

The external modes of the constituent ions are expected in the spectral region, 10−250 cm^{-1}.[41,43,45−47,52] Although assignment of the room temperature spectra has been attempted, the external modes are undoubtedly strongly coupled because of the inherent low symmetry, the high density of states, and the strong hydrogen bonding between the molecular groups. We are currently engaged in a normal coordinate analysis, which should facilitate assignment. Notwithstanding the complexity, this spectral region is of great value as it provides a fingerprint of the intermolecular bonding. Figure 1 presents spectra of the deuterated salt at 15 K and ambient pressure in the two structural forms, where the intensities have been normalized relative to the $\nu_1(SO_4)^{2-}$ Raman band. The switch of the long Cu−O bond and concomitant realignment of the sulfate and ammonium groups results in a dramatic change in the intensities and energies of the bands in this spectral region. Also shown in Figure 1 is the spectrum of the hydrogenous salt, exhibiting remarkable similarity to that of the switched deuterated salt in modification B. It has been suggested that deuteration may lead to a change in the anisotropic lattice strain acting on the copper(II) ion, by way of altering the hydrogen-bonding interactions,[21] but this is not supported by the Raman data presented. A reduction in the energies of the Raman bands is observed, on account of the increase in the reduced mass of the external modes that occurs upon deuteration.

3.2. Structural Determination of the Ammonium Copper Tutton Salts at 15 K. All the unit-cell lengths are longer in the hydrogenous salt, resulting in a ∼0.1% expansion of the unit-cell volume. The β angle is invariant. It is notable that a single-crystal X-ray diffraction study on the ammonium zinc Tutton salts revealed a similar change in the unit-cell

(37) Schoenitz, M.; Navrotsky, A.; Leinenweber, K. *Phys. Chem. Miner.* **2000**, *27*, 604.
(38) Best, S. P.; Beattie, J. K.; Armstrong, R. S. *J. Chem. Soc., Dalton Trans.* **1984**, 2611−2624.
(39) Armstrong, R. S.; Beattie, J. K.; Best, S. P.; Cole, B. D.; Tregenna-Piggott, P. L. W. *J. Raman Spectrosc.* **1995**, *26*, 921.
(40) Best, S. P.; Armstrong, R. S.; Beattie, J. K. *J. Chem. Soc., Dalton Trans.* **1992**, 299.
(41) Beattie, J. K.; Armstrong, R. S.; Best, S. P. *Spectrochim. Acta* **1996**, *51A*, 539−548.
(42) Gupta, S. P. G.; Khanna, B. N. *Indian J. Phys.* **1986**, *60B*, 347.
(43) Sekar, G.; Ramakrishnan, V.; Aruldhas, G. *J. Solid State Chem.* **1988**, *74*, 424.
(44) Gupta, S. P.; Kuar, Y.; Khanna, B. N. *Pramana.* **1991**, *36* (2), 151.
(45) Rajagopal, P.; Aruldhas, G. *J. Solid State Chem.* **1989**, *80*, 303.
(46) Barashkov, M. V.; Zazhogin, A. A.; Komyak, A. I.; Shashkov, S. N. *J. Appl. Spectrosc.* **2000**, *67* (4), 605.
(47) James, D. W.; Whitnall, J. M. *J. Raman. Spectrosc.* **1978**, *7* (4), 225.
(48) Ananthanarayanan, V.; Danti, A. *J. Mol. Spectrosc.* **1966**, *20*, 88.
(49) Ananthanarayanan, V. *Z. Phys.* **1961**, *163*, 144.
(50) Ananthanarayanan, V. *Z. Phys.* **1962**, *166*, 318.
(51) Ananthanarayanan, V. *J. Chem. Phys.* **1968**, *48* (2), 573.
(52) Singh, B.; Gupta, S. P.; Khanna, B. N. *Pramana* **1982**, *18* (5), 427.

Table 2. Comparison of Selected Bond Lengths and Angles[a]

Bond Lengths

bond	deuterate	hydrogenous	Δ	error	σ	bond	deuterate	hydrogenous	Δ	error	σ
Cul−O7	2.2802(4)	2.2834(5)	−0.0032	0.00064	**5.0**	O8−H17	0.9859(5)	0.9894(12)	−0.0035	0.00130	2.7
Cu1−O8	2.0082(4)	2.0077(5)	0.0005	0.00064	0.8	O8−H18	0.9816(5)	0.9818(13)	−0.0002	0.00139	0.1
Cu1−O9	1.9781(4)	1.9792(5)	−0.0011	0.00064	1.7	O9−H19	0.9770(7)	0.9800(14)	−0.0030	0.00157	1.9
S2−O3	1.4898(9)	1.4889(11)	0.0009	0.00142	0.6	O9−H20	0.9811(5)	0.9840(12)	−0.0029	0.00130	2.2
S2−O4	1.4657(9)	1.4669(11)	−0.0012	0.00142	0.8	N10−H11	1.0236(5)	1.0227(12)	0.0009	0.00130	0.7
S2−O5	1.4827(8)	1.4849(10)	−0.0022	0.00128	1.7	N10−H12	1.0208(5)	1.0188(14)	0.0020	0.00149	1.3
S2−O6	1.4829(9)	1.4832(12)	−0.0003	0.00150	0.2	N10−H13	1.0285(6)	1.0308(16)	−0.0023	0.00171	1.3
O7−H15	0.9711(5)	0.9691(13)	0.0020	0.00139	1.4	N10−H14	1.0309(5)	1.0313(13)	−0.0004	0.00139	0.3
O7−H16	0.9682(7)	0.9687(16)	−0.0005	0.00175	0.3						

Bond Angles

bond	deuterate	hydrogenous	Δ	error	σ	bond	deuterate	hydrogenous	Δ	error	σ
O7−Cu1−O8	89.08(1)	89.14(2)	−0.06	0.022	2.7	Cu1−O8−H17	114.61(4)	114.73(8)	−0.12	0.089	1.3
O7−Cu1−O9	90.65(1)	90.65(2)	0.00	0.022	0.0	Cu1−O8−H18	114.05(4)	114.09(8)	−0.04	0.089	0.4
O8−Cu1−O9	88.70(2)	88.79(2)	−0.09	0.028	**3.2**	H17−O8−H18	106.59(5)	106.78(11)	−0.19	0.121	1.6
O3−S2−O4	109.67(5)	109.75(7)	−0.08	0.086	0.9	Cu1−O9−H19	114.64(4)	114.73(8)	−0.09	0.089	1.0
O3−S2−O5	108.14(5)	108.11(7)	0.03	0.086	0.3	Cu1−O9−H20	118.32(4)	118.35(8)	−0.03	0.089	0.3
O3−S2−O6	108.86(5)	108.91(7)	−0.05	0.086	0.6	H19−O9−H20	104.87(5)	104.97(12)	−0.10	0.130	0.8
O4−S2−O5	109.33(6)	109.27(7)	0.06	0.092	0.7	H11−N10−H12	110.77(5)	110.95(13)	−0.18	0.139	1.3
O4−S2−O6	110.87(5)	110.88(7)	−0.01	0.086	0.1	H11−N10−H13	107.58(4)	107.42(11)	0.16	0.117	1.4
O5−S2−O6	109.93(5)	109.88(7)	0.05	0.086	0.6	H11−N10−H14	108.68(4)	108.57(12)	0.11	0.126	0.9
Cu1−O7−H15	109.92(4)	110.02(8)	−0.10	0.089	1.1	H12−N10−H13	109.08(5)	109.16(12)	−0.08	0.130	0.6
Cu1−O7−H16	114.01(4)	113.90(9)	0.11	0.098	1.1	H12−N10−H14	110.45(5)	110.31(11)	0.14	0.121	1.2
H15−O7−H16	107.35(5)	107.44(12)	−0.09	0.130	0.7	H13−N10−H14	110.23(5)	110.39(11)	−0.16	0.121	1.3

[a] Differences are deuterate − hydrogenous. All units are in Å and deg, respectively. Differences above three esd are indicated in bold type.

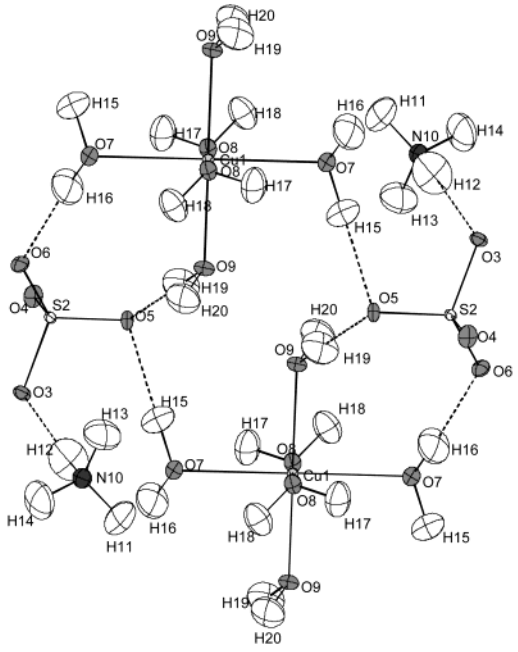

Figure 2. Switched deuterate structure of ammonium copper sulfate (form B), showing two copper centers with the surrounding hydrogen-bonding network. Thermal ellipsoids drawn at the 90% probability level.

volume upon deuteration.[53] Fractional coordinates and anisotropic displacement parameters are presented in Supporting Information S1 and S2. Table 2 lists the bond lengths of interest of both the hydrogenous and deuterated compounds, their differences, and significance. The molecular units comprising the structure are shown in Figure 2.

It is seen from Table 2 that the relative dispositions of the molecular groups are very similar for both structures. Differences in a given geometric parameter greater than 3 esd's are highlighted, and these are few. The most notable difference is found for the Cu−O(7) bond length, with the hydrogenous compound being 0.0032(6)Å longer than the deuterated salt. Smaller differences in O−Cu−O bond angles are also found with the O(7)−Cu−O(8) and O(8)−Cu−O(9) angles being larger by 2.7 and 3.2 esd's, respectively, in the hydrogenous salt.

The hydrogen-bonding network in the Tutton salts is extensive, and the observed pattern is as anticipated. Each ligated water has two hydrogen bonds to separate sulfate groups. In turn, each N−H of the ammonium cation is also hydrogen bonded to a sulfate oxygen. Parameters pertaining to hydrogen bonding are listed in Table 3 and suggest a greater variance in this network than in the formal bonding. Around the ammonium cation the N(10)···O(3) and H(12)···O(3) distances are longer in the hydrogenous salt, with $\sigma_{diff} > 3.0$. Conversely, the hydrogen bonds from the O(8) and O(9) water molecule are a little longer in the deuterated salt. The N(10)−H(11)···O(6) angle is larger in the hydrogenous salt with $\sigma_{diff} = 4.7$.

Statistically, differences with $\sigma_{diff} > 3.0$ may be considered significant. However, the fractional coordinates of the non-hydrogen atomic positions of the 15 K hydrogenous salt are not all within the experimental uncertainty of those published from a 9.5 K X-ray crystallographic study on the same compound.[21] Furthermore, the values of σ_{diff} are obtained by dividing small differences by very small errors. Further examination of the validity of our estimated uncertainties in the observed squared structure amplitudes, and estimation of the significance of the differences between the two structures, can be made by inspection of normal probability plots.[54,55] For the former, values of $\delta R = (F_{obs}^2 - F_{calc}^2)/\sigma(F_{obs}^2)$ are compared with the expected normal distribution;

(53) Simmons, J. C.; Hitchman, M. A.; Stratemeier, H. *Inorg. Chem.* **2000**, *39*, 6124.

Table 3. Hydrogen Bond Lengths and Differences[a]

Do−H···Ac	Do−X	Δ Do−X	σ	Do−Ac	Δ Do−Ac	σ	X···Ac	Δ X···Ac	σ	Do−X···Ac	Δ Do−X···Ac	σ
N10−H11···O6	1.0236(5)	0.0009(13)	0.69	2.8893(4)	0.0011(7)	1.5	1.9168(5)	0.0028(14)	2.0	157.54(4)	−0.55(12)	**4.7**
	1.0227(12)			2.8882(6)			1.9140(13)			158.09(11)		
N10−H12···O3	1.0208(5)	0.0020(15)	1.4	2.9825(5)	−0.0023(8)	2.9	2.0174(6)	−0.0046(15)	**3.0**	156.70(5)	0.06(14)	0.43
	1.0188(14)			2.9848(6)			2.0220(14)			156.64(13)		
N10−H13···O3	1.0285(6)	−0.0023(17)	1.4	2.8921(6)	−0.0036(9)	**3.9**	1.8729(7)	−0.0021(17)	1.2	170.37(4)	0.36(13)	2.9
	1.0308(16)			2.8957(7)			1.8750(16)			170.01(12)		
N10−H14···O5	1.0309(5)	−0.0004(14)	0.29	2.8457(4)	−0.0001(7)	0.14	1.8199(6)	0.0008(14)	0.56	172.89(5)	−0.31(12)	2.6
	1.0313(13)			2.8458(6)			1.8191(13)			173.20(11)		
O7−H15···O5	0.9711(5)	0.0020(14)	1.4	2.8412(5)	−0.0002(9)	0.21	1.8871(6)	−0.0023(14)	1.6	166.78(5)	0.04(12)	0.33
	0.9691(13)			2.8414(8)			1.8894(13)			166.74(11)		
O7−H16···O6	0.9682(7)	−0.0005(17)	0.29	2.8320(6)	−0.0014(11)	1.3	1.8894(7)	−0.0011(17)	0.63	163.77(5)	0.05(13)	0.38
	0.9687(16)			2.8334(9)			1.8905(16)			163.72(12)		
O8−H17···O4	0.9859(5)	−0.0035(13)	2.7	2.6756(5)	0.0012(9)	1.4	1.6897(6)	0.0046(13)	**3.4**	179.26(5)	−0.04(13)	0.31
	0.9894(12)			2.6744(7)			1.6851(12)			179.30(12)		
O8−H18···O6	0.9816(5)	−0.0002(14)	0.14	2.7193(5)	0.0019(9)	2.2	1.7386(5)	0.0022(13)	1.7	177.00(4)	0.01(12)	0.09
	0.9818(13)			2.7174(7)			1.7364(12)			176.99(11)		
O9−H19···O5	0.9770(7)	−0.0030(16)	1.9	2.7327(6)	−0.0008(10)	0.80	1.7663(6)	0.0018(15)	1.2	169.54(5)	0.25(13)	1.9
	0.9800(14)			2.7335(8)			1.7645(14)			169.29(12)		
O9−H20···O3	0.9811(5)	−0.0029(13)	2.2	2.6951(5)	0.0011(9)	1.3	1.7233(5)	0.0040(13)	**3.1**	170.09(4)	−0.05(12)	0.43
	0.9840(12)			2.6940(7)			1.7193(12)			170.14(11)		

[a] The upper value corresponds to the distance or angle in the switched deuterated salt (form B), whereas the lower value is the hydrogenous value. **Do** indicates the donor atom, **X** indicates either the hydrogen or deuterium, and **Ac** indicates the acceptor. Differences are deuterate − hydrogenous. All units are in Å or deg, respectively. Differences above three esd are indicated in bold type.

for the latter, differences Δp between pairs of supposedly identical coordinates or derived quantities (e.g., bond lengths or angles) are examined in a $\delta p = |\Delta p|/\sigma(\mathrm{p})$ half-normal probability plot. δR plots (not shown) after the final refinements show that our estimated uncertainties in the observed squared structure amplitudes in both sets of data are slightly underestimated (this is also evident in the S values quoted in Table 1). However, adjusting the uncertainties via the parameters c_1 and c_2 and $\sigma'(F_{\mathrm{obs}}^2) = [\{c_1\sigma(F_{\mathrm{obs}}^2)\}^2 + \{c_2F_{\mathrm{obs}}^2\}^2]^{1/2}$ to give δR normal-probability plots as nearly linear as possible with a slope of 1.0 changes the parameters in both sets of data by less than 10% of their estimated uncertainties and the uncertainties themselves by less than 1%. We can therefore accept the parameters and estimated uncertainties given in Table 2. Although the two structures are not expected to be identical, we can still compare them via δp plots on the sets of bond lengths and angles listed in Table 2. Figure 3 shows that the bond length Cu−O7 is clearly anomalous, the angles O7−Cu−O8 and O8−Cu−O9 are possibly anomalous, whereas the remaining bond lengths and angles are normally distributed, albeit with slightly underestimated uncertainties if the structures should be identical. We thus conclude that the estimated uncertainties in our final parameters are reasonably correct and that the difference between the Jahn−Teller distortions in the two structures is real. We note that a δp plot based on our coordinates of non-H atoms and those of the 9.5 K X-ray structure[21] is quite linear, although the slope of 2.6 does indicate that the combined uncertainties are somewhat underestimated. In the next section we explore the implications of structural differences with $\sigma_{\mathrm{diff}} > 3.0$.

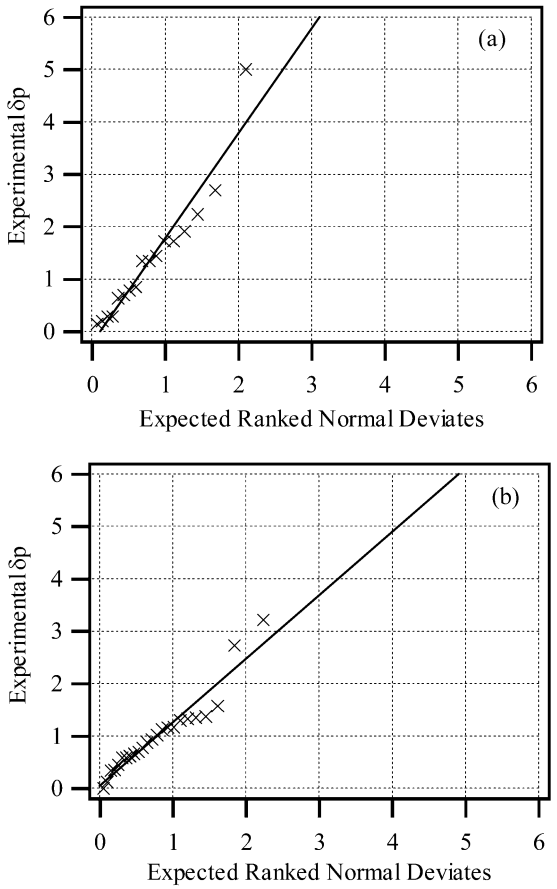

Figure 3. δp half-normal probability plots for (a) the bond lengths and (b) the bond angles listed in Table 2. The outliers correspond to the Cu−O7 length, and the O7−Cu−O8 and O8−Cu−O9 angles.

3.3. Calorimetric Measurements. DSC measurements on switched $(ND_4)_2Cu(OD_2)_6(SO_4)_2$ (form B) exhibited an extremely rapid exothermic phase transition, and a representative curve is shown in Figure 4. The phase transition was observable as the crystal disintegrated with an audible "click". A total of 10 repeated measurements on single-crystal pieces, between 1 and 26 mg, gave a transition temperature of 295.8(5) K and an enthalpy of 0.41(4) J/g.

(54) Abrahams, S. C.; Keve, E. T. *Acta Crystallogr.* **1971**, *A27*, 157.
(55) Hamilton, W. C.; Abrahams, S. C. *Acta Crystallogr.* **1972**, *A28*, 215.

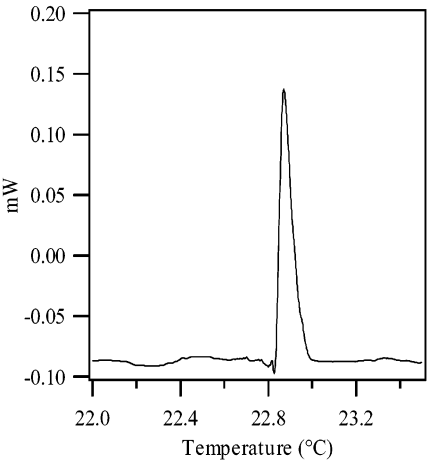

Figure 4. Representative DSC plot showing the exothermic phase transition of $(ND_4)_2Cu(OD_2)_6(SO_4)_2$ from the B form back to the A form. Heating rate of 0.5 °C/min, data interval of 0.1 pt/s.

The relatively large variation in integrated enthalpy is thought to stem, in part, from the poor thermal contact that occurs when the crystal violently disintegrates. The crystal history possibly also plays a significant role, with cutting altering the strain at the crystal periphery. However, as-grown single crystals showed no discernible difference, within the reproducibility of the experiment, compared to the cut samples. The DSC measurements provide the most direct measure of the enthalpy change that accompanies the phase transition to date. The result of 0.17(2) kJ/mol demonstrates that at room temperature the enthalpy difference between the two structural forms is extremely small. It is for this reason that the salt may be switched to form B by perturbations such as isotopic substitution, or doping with Zn^{2+}.

4. Discussion

The differences in the Cu−O bond lengths between the two structures can be conveniently represented in terms of displacements along the internal coordinates of the CuO_6 framework. Because the hexaaqua cation is centrosymmetric, we need only consider the *gerade* CuO_6 stretching vibrations $\nu_1[CuO_6]$ and $\nu_2[CuO_6]$ with transformation properties $Q_a^s \approx \Delta z^2 + \Delta x^2 + \Delta y^2$ and $Q_\theta^s \approx 2\Delta z^2 - \Delta x^2 - \Delta y^2$, $Q_\epsilon^s \approx \sqrt{3}(\Delta x^2 - \Delta y^2)$, respectively. Displacements along these coordinates may be expressed in a basis of increments in the metal−oxygen bond lengths: $\mathbf{Q_a}^s = \rho_{\nu 1}(1/\sqrt{6})(\mathbf{r}_1 + \mathbf{r}_4 + \mathbf{r}_2 + \mathbf{r}_5 + \mathbf{r}_3 + \mathbf{r}_6)$; $\mathbf{Q_{e\theta}}^s = \rho_{\nu 2} \cos \phi_{\nu 2} (1/\sqrt{12})(2\mathbf{r}_1 + 2\mathbf{r}_4 - \mathbf{r}_2 - \mathbf{r}_5 - \mathbf{r}_3 - \mathbf{r}_6)$; $\mathbf{Q_{e\epsilon}}^s = \rho_{\nu 2} \sin \phi_{\nu 2}\ ^1/_2(\mathbf{r}_2 + \mathbf{r}_5 - \mathbf{r}_3 - \mathbf{r}_6)$, where $\mathbf{r}_i$ is a unit displacement along the M−O_i bond vector. The bond length displacements, Δr_i, are then related to $\rho_{\nu 1}$, $\rho_{\nu 2}$, and $\phi_{\nu 2}$ as follows:

$$\Delta r_1 = \Delta r_4 = \frac{\rho_{\nu 2}}{\sqrt{12}}(2\cos\phi_{\nu 2}) + \frac{\rho_{\nu 1}}{\sqrt{6}}$$

$$\Delta r_2 = \Delta r_5 = \frac{\rho_{\nu 2}}{\sqrt{12}}(-\cos\phi_{\nu 2} + \sqrt{3}\sin\phi_{\nu 2}) + \frac{\rho_{\nu 1}}{\sqrt{6}} \quad (1)$$

$$\Delta r_3 = \Delta r_6 = \frac{\rho_{\nu 2}}{\sqrt{12}}(-\cos\phi_{\nu 2} - \sqrt{3}\sin\phi_{\nu 2}) + \frac{\rho_{\nu 1}}{\sqrt{6}}$$

Table 4. Displacements of the $[Cu(OH_2)_6]^{2+}$ and $[Cu(OD_2)_6]^{2+}$ Cations along the $\nu_1(CuO_6)$ and $\nu_2(CuO_6)$ Stretching Coordinates[a]

	deuterate	hydrogenous
$\rho_{\nu 1}$ (Å)	zero by definition	0.0031(6)
$\rho_{\nu 2}$ (Å)	0.3328(5)	0.3360(6)
$\phi_{\nu 2}$ (deg)	245.2(1)	244.9(1)

[a] The quantities $\rho_{\nu 1}$, $\rho_{\nu 2}$, and ϕ_{N2} were calculated using eq 1. The displacements are relative to the average Cu−OD_2 bond length.

Values of $\rho_{\nu 1}$, $\rho_{\nu 2}$, and $\phi_{\nu 2}$ for the hydrogenous and deuterated salts are given in Table 4. In both cases the displacements are calculated relative to the average Cu−OD_2 bond length. The values of $\rho_{\nu 2}$ and $\rho_{\nu 1}$ for the hydrogenous salt are a little larger than the values for the deuterated counterpart with $[\rho_{\nu 2}(H) - \rho_{\nu 2}(D)] = 0.0032(8)$ Å and $[\rho_{\nu 1}(H) - \rho_{\nu 1}(D)] = 0.0031(8)$ Å. Both values of $\rho_{\nu 2}$ are considerably smaller than the value of 0.369(3) Å, determined for the deuterated salt in modification A, at 15 K.[2] No significant change in $\phi_{\nu 2}$ is identified, being 245.2(1)° and 244.9(1)° for the deuterated and hydrogenous salts, respectively.

Small differences in the expectation value, $\rho_{\nu 2}$, between the hydrogenous and deuterated salts are to be expected, purely on the basis of anharmonicity in the E⊗e potential energy surface combined with differences in the zero-point energies. This contribution can be addressed experimentally and theoretically.[8,62] The change in the mass of the water molecules upon deuteration may also be achieved by substitution of ^{18}O for ^{16}O; therefore, the decrease in the zero-point energies of the $[Cu(OH_2)_6]^{2+}$ stretching vibrations is also identical. In the present study, small differences in a number of bond distances and bond angles have been determined, whereas in the 9.5 K X-ray determination of the hydrogenous and ^{18}O enriched salts,[21] all the bond angles and bond distances are identical within the 3 esd limit. Specifically, Cu−$D_2O(7)$ − Cu−$H_2O(7)$ is determined as −0.0032(6) Å from the present 15 K study, whereas Cu−$H_2{}^{18}O(7)$ − Cu−$H_2{}^{16}O(7)$ was determined to be +0.0011(12) Å from the 9.5 K X-ray study. Using the most recent vibronic coupling parameters proffered for this system,[15] a contour plot of the potential energy in the $^2E\otimes e$ subspace can be generated, and this is shown in Figure 5a. Low symmetry strain lifts the degeneracy of the three potential minima, and at 15 K only the population of the lowest-lying potential well is significant. Figure 5b shows a cross-section of the potential energy surface, with the ground-state probability density, along the path which includes the potential energy minimum, indicated by the gray line in Figure 5a. Although the lowest potential well appears

(56) Ham, F. S. *Phys. Rev.* **1968**, *166*, 307.
(57) Rundle, R. E. *J. Phys.* **1964**, *25*, 187.
(58) Falk, M.; Knop, O. Water in Stoichiometric Hydrates. In *Water, a Comprehensive Treatise*; Franks, F., Ed.; Plenum Press: New York, 1973; Chapter 2, pp 55−113.
(59) Armstrong, R. S.; Beattie, J. K.; Best, S. P.; Skelton, B. W.; White, A. H. *J. Chem. Soc., Dalton Trans.* **1983**, 1973.
(60) Beattie, J. K.; Best, S. P.; Skelton, B. W.; White, A. H. *J. Chem. Soc., Dalton Trans.* **1983**, 2105.
(61) Best, S. P.; Armstrong, R. S.; Beattie, J. K. *J. Chem. Soc., Dalton Trans.* **1982**, 1655.
(62) Tregenna-Piggott, P. L. W. *Advances in Quantum Chemistry*, in press.

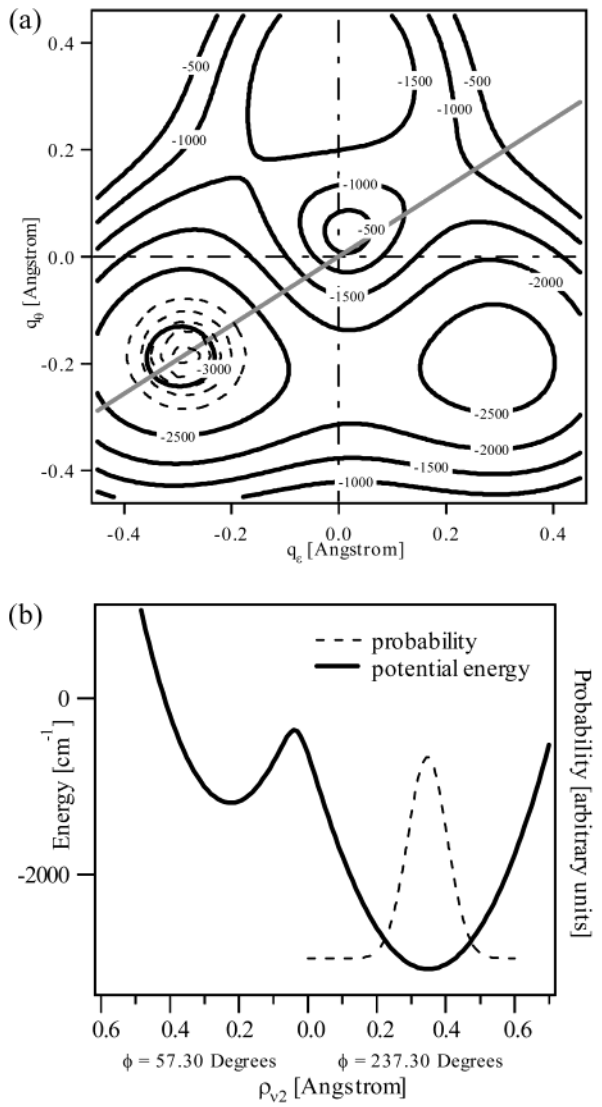

Figure 5. (a) Contour plots of the potential energy surface, in wavenumbers, and the probability density of the lowest eigenstate as functions of q_ϵ and q_θ, represented by bold and dashed contours, respectively. (b) Cross-section through the potential energy surface and probability density function, corresponding to the gray line in (a).

symmetric, the surface does actually rise more steeply on the side of *higher* ρ_{v2} than of *lower* ρ_{v2}. When the ground-state functions of the hydrogenous and deuterated Cu(II) aqua ions are compared, the hydrogenous probability density is more diffuse, and is centered at slightly *lower* ρ_{v2}. The expectation value, ρ_{v2}, for the $[Cu(OH_2)_6]^{2+}$ cation in the two-dimensional coordinate space is ~0.0003 Å *less* than the $[Cu(OD_2)_6]^{2+}$ cation. We have repeated the calculation for other values of the vibronic coupling coefficients and have obtained similar results. It may be concluded that the observed increase in ρ_{v2} upon substitution of hydrogen for deuterium is due to a change in the parameters which define the average, effective potential experienced by the hexaaqua ion in the crystal environment. Such a change in the effective potential would have to be related to a change in the effective hydrogen-bonding interactions brought about by isotopic substitution.

At low temperatures, the value of ρ_{v2} approximates to the displacement of the potential-energy minimum along the ν_2-$[CuO_6]$ coordinate: the Jahn−Teller radius. To first-order in the Jahn−Teller coupling interaction, the stabilization energy, E_{JT}, the coupling constant, V, the force constant, F, and the Jahn−Teller radius, R_{JT} are related by the following equations,[56]

$$E_{JT} = \frac{V^2}{2F}; \quad R_{JT} = \frac{V}{F} \tag{2}$$

In the copper(II) Tutton salts the situation is far more complicated, with higher-order effects and low symmetry strain making a significant contribution to the geometry and stability of the molecule.[8] Nevertheless, it is generally the case that the greater the value of R_{JT}, the greater the value of E_{JT}. The value of R_{JT} depends on the nature of the chemical bonding and not on the mass of the ligand as stated in ref 18. Differences in ρ_{v1} and ρ_{v2} are consistent with changes in the $\nu_1[CuO_6]$ and $\nu_2[CuO_6]$ force constants. A significant change in the nature of the anisotropic lattice strain would give rise to a change in the value of ϕ_{v2} and in the low-wavenumber Raman spectra, neither of which is observed.

Changes in the effective force field about the copper(II) hexaaqua cation in the two structures can arise as a direct or indirect consequence of changes to the hydrogen bonding, which are often observed to occur upon deuteration, on account of the large change in the zero-point energy of the hydrogen bonds.[58,57] This isotope effect normally manifests itself in shorter hydrogen bonds in the range of 2.5−2.7 Å, whereas in longer hydrogen bonds in the range of 2.7−2.9 Å, the observed changes are usually quite small, about the same magnitude as the experimental error.[58] The structural data do indeed suggest some differences in some of the hydrogen bond lengths (Table 3), particularly those arising from the ammonium group. The overall effect of many small differences in bond angles and lengths, particularly the hydrogen bonding between the molecular group, reduces the unit-cell volume for the deuterated salt by 0.92(14) Å^3. Raman and structural studies of the alums have shown that the denser the packing of the constituent molecular groups, the greater the force constants of the intramolecular vibrations.[59−61] Thus, the changes in the Cu−O bond lengths and in the unit-cell size both suggest a slight increase in the force field about the copper(II) center in the deuterated salt, leading to smaller values of ρ_{v1} and ρ_{v2}. This could, in principle, be verified from a detailed analysis of the Raman spectra, which we are currently undertaking.

The quantities E_{JT} and ρ_{v2} may be interrelated by numerical solution of the vibronic Hamiltonian, as described previously.[15,62,63] We calculate that the slight increase in ρ_{v2} upon substitution of deuterium by hydrogen is consistent with an increased stabilization of ~0.3 kJ/mol, by way of a slight reduction in the force constant; that is, if the deuterated salt were to crystallize in modification B, then the contribution of the Jahn−Teller stabilization energy to the free energy

(63) Dobe, C.; Andres, H.; Tregenna-Piggott, P. L. W.; Mossin, S.; Weihe, H.; Janssen, S. *Chem. Phys. Lett.* **2002**, *362*, 387.

of the salt would be slightly less than in the hydrogenous counterpart. The difference in ρ_{v2} is very small, however, especially when compared to the difference in the values determined for the deuterated salt in the two structural forms.[2,18]

The focus of our attention has been on the Jahn−Teller stabilization energy as this quantity is extremely sensitive to small perturbations of the crystal lattice and, for copper(II) salts, makes a significant contribution to the overall free energy. A more rigorous treatment would be to undertake ab initio calculations on a fragment of the unit cell, to assess the significance of the small changes in the hydrogen-bonding network. However, given that the structural differences are so tiny, and having recently been engaged in density functional theory calculations on hexaaqua cations,[64] we believe that the theoretical approaches commonly employed to assess the stability of solid structures are not at the degree of sophistication to be of any value to the current problem.

A detailed analysis of the temperature dependence of the thermodynamic functions, ΔG, ΔH, and ΔS, and especially the vibrational contributions to these functions, might afford an alternative interpretation of the small energy difference between the hydrogenous and deuterated salts in modification B. This would require much more experimental information at the thermodynamical and lattice dynamical level than is presently available.

Finally, it should be emphasized that the foregoing discussion considers only half of the problem, as it is the stability of modification B, relative to A, that is the important quantity. Sadly, although it is possible to prepare the deuterated salt in both modifications, to the best of our knowledge, the hydrogenous salt can be prepared only in modification B.

5. Conclusions

Single-crystal Raman and neutron-diffraction studies of the hydrogenous ammonium copper Tutton salt, and the deuterated analogue in the metastable state, have revealed few structural differences. However, the unit-cell volume for the hydrogenous salt is 0.92(14) Å^3 larger than for the deuterate, and small but significant changes in the hydrogen-bonding contacts and in the geometry of the copper(II) hexaaqua cation are identified. It may be concluded that deuteration leads to changes in the hydrogen-bonding interactions, which impact upon the effective form of the E⊗e Jahn−Teller potential energy surface of the copper(II) hexaaqua cation. The small structural differences suggest different relative stabilities for the hydrogenous and deuterated salts in form B, which may be a factor in the hydrogenous salt being stable in this anomalous structural form.

Acknowledgment. We are indebted to Michael Hitchman for his encouragement, careful reading of the manuscript, and subsequent comments and suggestions. We are also indebted to him for providing a copy of a manuscript (ref 20) prior to publication. Our gratitude is also extended to Uli Kindler for constructing the pressure cell and Andreas Hauser for use of the He compressor. This work was funded by the Swiss National Science Foundation.

Supporting Information Available: Tables of fractional coordinates and thermal parameters. This material is available free of charge via the Internet at http://pubs.acs.org.

IC0343511

(64) Tregenna-Piggott, P. L. W.; Andres, H.; McIntyre, G. J.; Best, S. P.; Wilson, C. C.; Cowan, J. A. *Inorg. Chem.* **2003**, *42*, 1350.